GEOPHYSICS, VOL. 61, NO. 3 (MAY-JUNE 1996); P. 795-803, 7 FIGS.

# True-amplitude migration taking fine layering into account

C. P. A. Wapenaar* and F. J. Herrmann*

**ABSTRACT**

The central process in wave-equation- based depth migration is inverse wavefield extrapolation. The commonly applied matched filter approach to inverse wavefield extrapolation ignores the angle-dependent amplitude and phase distortions that are related to fine layering. This may result in dispersed images and erroneous amplitude variation with angle of incidence (AVA) effects.

"Power reciprocity" formulates a relation between transmitted and reflected wavefields. It provides the basis for a modified matched filter that does account for the aforementioned distortions. The correction term by which the matched filter is modified can be derived directly from the reflection data. With this modified matched filter, prestack depth migration will yield non-dispersed images with correct AVA behavior.

## INTRODUCTION

The reflection information in seismic measurements is blurred by the propagation effects between the surface and the reflecting boundaries. In seismic migration, one aims to image the reflection properties by eliminating the propagation effects from the seismic measurements. These propagation effects are generally quantified in terms of one-way wavefield propagators in a macro model (Berkhout, 1982). Consequently, the elimination of the propagation effects is accomplished by applying the inverse of these wavefield propagators to the seismic data. Generally these inverse propagators are approximated by taking the complex conjugate of the forward propagators (hereafter referred to as the matched filter approach). It can be shown that this approach yields accurate results both for homogeneous as well as inhomogeneous macro models with small contrasts (Berkhout, 1982; Wapenaar and Berkhout, 1989).

A migrated image reveals details on the order of half the seismic wavelength. Obviously, details at a smaller scale cannot be resolved. However, this does not mean that the effects of the small scale variations of the medium parameters should be ignored altogether.

Extensive studies on wave propagation through 1-D finely layered' media have shown that internal multiple scattering may seriously affect the apparent propagation properties of the seismic wavefield (see, for example, O'Doherty and Anstey, 1971; Hubral et al., 1980; Resnick et al., 1986; Burridge and Chang, 1989; Herrmann and Wapenaar, 1993). The main effect is an angle-dependent dispersion. Current macro models do not account for this effect. Consequently, this effect is also ignored in migration. This may result in dispersed images and erroneous amplitude variation with angle of incidence (AVA) effects.

In a companion paper (Wapenaar, 1996), we introduce the 3-D *generalized primary* representation of seismic reflection data [the notion generalized primary was introduced in Hubral et al. (1980) who used this term for reflection data from 1-D finely layered media]. Ideally, the 3-D generalized primary propagators in this representation are defined in an *extended* macro model that accounts for the angle-dependent dispersion related to the fine layering.

In its explicit form, the generalized primary representation is linear in the reflection operator. In this paper, we formulate true amplitude migration as a genuine linear inversion of the generalized primary representation. The main complication is that the matched filter approach cannot be used to approximate the inverse propagators. A modified matched filter will be proposed, based on a power reciprocity relation between flux normalized transmitted wavefields (the generalized primary propagator) and flux normalized reflected wavefields (the deconvolved seismic data).

[1] Fine layering means: layering at a scale smaller to much smaller than the seismic wave length (not necessarily 1-D).

Presented at the 63rd Annual International Meeting, Society of Exploration Geophysicists. Manuscript received by the Editor December 22, 1993; revised manuscript received August 14, 1995.
*Centre for Technical Geoscience, Laboratory of Seismics and Acoustics, Delft University of Technology, P.O. Box 5046, 2600 GA Delft, The Netherlands.

## THE GENERALIZED PRIMARY REPRESENTATION

Consider an acoustic medium in which the position is denoted by the Cartesian coordinate vector x = *(x, y, z),* with the z-axis pointing downward. We assume that the upper half-space $z \leq z_0$ is homogeneous; the lower half-space $z > z_0$ may be inhomogeneous. In this configuration, we consider flux-normalized one-way wavefields, represented in the angular frequency domain by $P^+$ (x) and $P^-$ (x), where the superscripts "+" and "-" denote downward and upward propagation, respectively. The frequency variable ω is suppressed for notational convenience. Consider a "one-way source" for downgoing wavefields at $x_s$ and a "one-way detector" for upgoing wavefields at $x_D$, both in the upper half-space; hence, $zs \leq z_0$ and $z_D \leq z_0$. We come back to the concept of one-way sources and detectors later on in this section. Now the upgoing wavefield $P^-(x_D)$ may be expressed in terms of the source $S_0^+(\mathbf{x}_S)$ for downgoing waves, according to

$$P^-(\mathbf{x}_D) = \int_\Omega W_g^-(\mathbf{x}_D, \mathbf{x})\hat{R}^+(\mathbf{x})W_g^+(\mathbf{x}, \mathbf{x}_S)S_0^+(\mathbf{x}_S)\, d^3\mathbf{x}, \tag{1a}$$

with

$$W_g^-(\mathbf{x}_D, \mathbf{x}) = W_g^+(\mathbf{x}, \mathbf{x}_D) \tag{1b}$$

(Wapenaar, 1996). Here Ω denotes the lower half-space $z > z_0$ ; $W_g^+$ (x, $x_s$ ) describes generalized downward propagation from $x_s$ to x, $\hat{R}^+$ (x) describes reflection at x, and $W_g^-$ ($x_D$ , x) generalized upward propagation from x to $x_D$, respectively (see Figure 1).

If we omit the subscripts g, then equation (1) would be nothing but an integral formulation of Berkhout's discrete representation of primary reflection data (Berkhout, 1982). In its present form, equation (1) is a representation of generalized primary reflection data. The generalized primary propagators $W_g^+$ and $W_g^-$ are one-way Green's functions defined in a configuration that is identical to the actual medium above depth level *z* and that is scatter-free below *z* (see Figure 1). Hence, $W_g^+$ and $W_g^-$ account for internal multiple reflections occurring in the region between $z_o$ and *z,* whereas reflections from the region below *z* are excluded. All internal multiple reflections occurring in the lower half-space Ω are included in $P^-$ ($x_D$ ) as a result of the integration along the depth coordinate *z.*

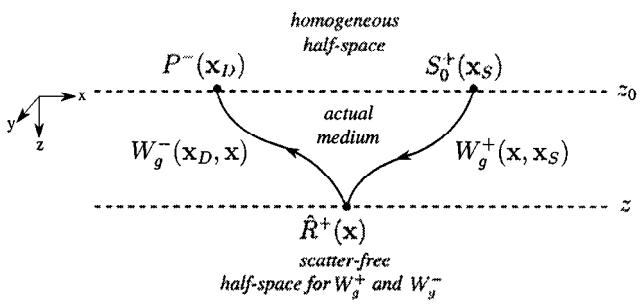


FIG. 1. The generalized primary representation.

Equation (1) applies to 3-D inhomogeneous media, including fine layering. For practical applications, $W_g^+$ and $W_g^-$ may either be parameterized or defined in an extended macro model (with anisotropic anelastic losses) that mimicks the effects of the fine layering. In both cases the fine layering is *upscaled* to macro parameters that describe the statistics of the fine layering. For laterally invariant media, these two approaches are discussed, in Herrmann and Wapenaar (1993) and Wapenaar et al. (1994). For 3-D inhomogeneous media, these approaches are currently under investigation.

In seismic practice, one-way sources and detectors do not exist. Moreover, instead of a homogeneous upper half-space $z \leq z_0$, the assumption of a free surface at *z.* would be more realistic. In two recent publications (Wapenaar and Berkhout, 1989; Verschuur et al., 1992), we discussed a surface-related preprocessing technique for decomposing seismic data at a free surface into downgoing and upgoing waves and for eliminating the surface-related multiple reflections. The situation after these preprocessing steps (one-way sources and detectors; free surface removed) matches the conditions for validating equation (1). In the remainder of this paper, we will assume that surface-related preprocessing has been applied so that equation (1) accurately describes the data.

## PRINCIPLE OF TRUE-AMPLITUDE MIGRATION

In its explicit form, the generalized primary representation is linear in the reflection operator $\hat{R}^+$ (x). True-amplitude migration is based essentially on inverting this representation for the reflection operator. The circumflex denotes that $\hat{R}^+$ (x) is a pseudodifferential operator that depends on the horizontal differentiation operators $\partial/\partial x$ and $\partial/\partial y$. In the following, we write x = ($x_H$, *z),* where $x_H$ contains the horizontal coordinates, according to $x_H$ = (x, y). If we replace $\hat{R}$ + ($x_H$, *z)* by its kernel R + ($x_H$, *z;* $\mathbf{x}'_H$), equation (1) may be rewritten as

$$P^-(\mathbf{x}_D) = \int_{z_0}^{\infty} dz \int_{\mathcal{R}^2} d^2\mathbf{x}_H W_g^-(\mathbf{x}_D; \mathbf{x}_H, z)$$

$$\times \int_{\mathcal{R}^2} d^2\mathbf{x}'_H R^+(\mathbf{x}_H, z; \mathbf{x}'_H)W_g^+(\mathbf{x}'_H, z; \mathbf{x}_S)S_0^+(\mathbf{x}_S). \tag{2}$$

To formulate the migration problem more conveniently, we adopt Berkhout's discrete notation. For equation (2) this yields

$$\mathbf{P}^-(z_D) = \underline{\mathbf{X}}_0(z_D, z_S)\mathbf{S}_0^+(z_S), \tag{3a}$$

with the one-way response matrix $\underline{\mathbf{X}}_0(z_D, z_S)$ defined by

$$\underline{\mathbf{X}}_0(z_D, z_S) = \sum_{n=1} \underline{\mathbf{W}}_g^-(z_D, z_n)\underline{\mathbf{R}}^+(z_n)\underline{\mathbf{W}}_g^+(z_n, z_S), \tag{3b}$$

with

$$\underline{\mathbf{W}}_g^-(z_D, z_n) = \{\underline{\mathbf{W}}_g^+(z_n, z_D)\}^T, \tag{3c}$$

where *T* denotes transposition. Each column in any of the matrices represents (one frequency component of) a discretized impulse response. See Figure 2 for a visualization of $\underline{\mathbf{W}}_g^+$ and $\underline{\mathbf{X}}_0$ for the special case of a 2-D medium. The summation in equation (3b) accounts for the integral along *z* in equation (2). The matrix product $\underline{\mathbf{R}}^+(z_n)\underline{\mathbf{W}}_g^+(z_n, z_S)$ accounts

for the 2-D integration in equation (2) with respect to $\mathbf{x}'_H$ for fixed $z = z_n$; the matrix product $\underset{\sim}{\mathbf{W}}_g^-(z_D, z_n)\underset{\sim}{\mathbf{R}}^+(z_n)$ accounts for the 2-D integration with respect to $x_H$ for fixed $z = z_n$. Actually the matrix-vector product $\underset{\sim}{\mathbf{X}}_0(z_D, z_S)\mathbf{S}_0^+(z_S)$ also describes a 2-D integration. In equation (2), this integral is absent since the source is represented by a spatial delta function. This implies that the source vector $\mathbf{S}_0^+(z_s)$ in equation (3a) contains one nonzero element only. The vector P- $(z_D)$ in equation (3a) contains $P$- $(x_D)$ for all $x_D$ with $z_D$ fixed. Hence, equation (3) describes all the data (for one frequency component) in a preprocessed seismic shot record. In the following, we choose for convenience $z_s = z_D = z_0$. All the data (for one frequency component) in a preprocessed seismic survey can thus be combined in one equation as follows

$$\underset{\sim}{\mathbf{P}}^-(z_0) = \underset{\sim}{\mathbf{X}}_0(z_0, z_0)\underset{\sim}{\mathbf{S}}_0^+(z_0), \tag{4}$$

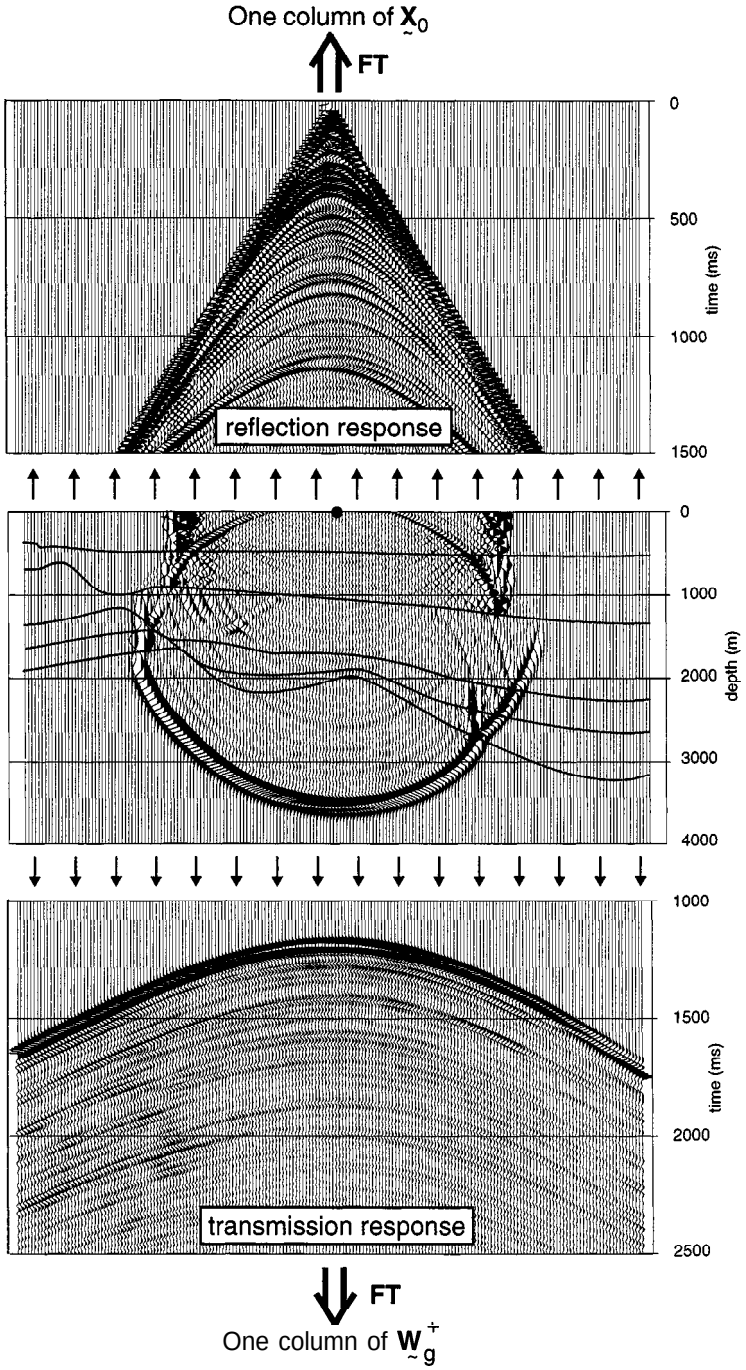


FIG. 2. Schematic presentation of some matrices appearing in equation (3). The source is a band-limited delta function. FT stands for a Fourier transform from $t$ to $\omega$. (The medium in the middle frame contains macro layers as well as fine layering; only the macro boundaries are shown).

where each column of $\underline{\mathbf{P}}^-(z_0)$ contains a data vector (i.e., a shot record) $P^-(z_0)$ and where each column of $\underline{\mathbf{S}}_0^+(z_0)$ contains a source vector $\mathbf{S}_0^+(z_0)$ with one nonzero element. By properly ordering the source vectors, we may write

$$\underline{\mathbf{S}}_0^+(z_0) = \underline{\mathbf{I}} S(\omega), \tag{5}$$

where $\underline{\mathbf{I}}$ is the identity matrix and $S(\omega)$ is (one frequency component of) the source spectrum. With this formulation, true amplitude migration involves the following steps:

1) Compensation for the source spectrum ("deconvolution"), according to

$$\underline{\mathbf{X}}_0(z_0, z_0) = S^{-1}(\omega)\underline{\mathbf{P}}^-(z_0). \tag{6}$$

2) Downward extrapolation to any depth level $z = z_m$, according to

$$\underline{\mathbf{X}}_0(z_m, z_m) = \underline{\mathbf{F}}_g^-(z_m, z_0)\underline{\mathbf{X}}_0(z_0, z_0)\underline{\mathbf{F}}_g^+(z_0, z_m), \tag{7}$$

where

$$\underline{\mathbf{F}}_g^+(z_0, z_m) = \{\underline{\mathbf{W}}_g^+(z_m, z_0)\}^{-1} \tag{8a}$$

and

$$\underline{\mathbf{F}}_g^-(z_m, z_0) = \{\underline{\mathbf{W}}_g^-(z_0, z_m)\}^{-1}. \tag{8b}$$

Note that

$$\underline{\mathbf{F}}_g^-(z_m, z_0) = \{\underline{\mathbf{F}}_g^+(z_0, z_m)\}^T \tag{8c}$$

because of equation (3c). Numerical inversion of the matrices $\underline{\mathbf{W}}_g^+$ and $\underline{\mathbf{W}}_g^-$ is very unstable and should be avoided at all costs. This will be discussed again later in the paper.

3) Imaging at any depth level $z = z_m$, according to

$$\underline{\mathbf{X}}_0(z_m, z_m) \rightarrow \underline{\mathbf{R}}^+(z_m) \tag{9}$$

in some sense. Here a straightforward integration with respect to $\omega$ is not sufficient for obtaining the true-amplitude, angle-dependent reflectivity at depth level $z_m$. Imaging for angle-dependent reflectivity is amply discussed in de Bruin et al. (1990) and Wapenaar et al. (1995) and will not be discussed in this paper any further.

Downward extrapolation (step 2) is the central process in this (and any other) depth migration scheme. It involves inversion of the generalized primary propagators $\underline{\mathbf{W}}_g^+$ and $\underline{\mathbf{W}}_g^-$. The dispersion effects in these propagators are accompanied with a frequency-dependent amplitude loss that is not compensated for by the matched filter approach. Hence, just as is the case with anelastic losses, the matched filter fails to account for losses that are related to the fine layering. There is an important difference, however, between anelastic losses and losses related to fine layering. Whereas anelastic losses represent a conversion of seismic energy into heat, the "losses" related to fine layering represent a conversion of forward propagating seismic energy into backscattered seismic energy (see Figure 2) (henceforth we will speak of scattering losses). Moreover, whereas the (approximately) angle independent anelastic losses could be accounted for by a time-variant deconvolution process, the angle-dependent scattering losses require a more advanced approach. Looking at Figure 2, it may be clear that the scattering losses in $\underline{\mathbf{W}}_g^+$ can be quantified in terms of $\underline{\mathbf{X}}_0$, i.e., the deconvolved reflection response. We elaborate on "the quantification of the scattering loss," not on "the deconvolved reflection response." We will elaborate on this in the following two sections.

## POWER RECIPROCITY THEOREM FOR ONE-WAY WAVEFIELDS

We will use reciprocity to quantify the scattering losses and to derive simple explicit expressions for the inverse generalized primary propagators. In general, a reciprocity theorem interrelates the quantities that characterize two admissable physical states that could occur in one and the same domain in space-time (de Hoop, 1988). One can distinguish between convolution and correlation type reciprocity theorems (Bojarski, 1983; Fokkema and van den Berg, 1993). Generally the reciprocity theorems are formulated in terms of two-way (i.e., total) wavefields. Here we will use a correlation-type reciprocity theorem for *one-way* wavefields as the basis for deriving the inverse wavefield propagators $\underline{\mathbf{F}}_g^+(z_0, z_m)$ and $\underline{\mathbf{F}}_g^-(z_m, z_0)$. In the Appendix, we derive for the configuration of Figure 3

$$\int_{\Sigma_0} (\{P_A^+(\mathbf{x})\}^* P_B^+(\mathbf{x}) - \{P_A^-(\mathbf{x})\}^* P_B^-(\mathbf{x}))\, d^2\mathbf{x}_H$$

$$= \int_{\Sigma_m} (\{P_A^+(\mathbf{x})\}^* P_B^+(\mathbf{x}) - \{P_A^-(\mathbf{x})\}^* P_B^-(\mathbf{x}))\, d^2\mathbf{x}_H, \tag{10}$$

where * denotes complex conjugation and where $\Sigma_0$ and $\Sigma_m$ denote horizontal depth levels defined by $z = z_0$ and $z = z_m$, respectively. The subscripts $A$ and $B$ refer to the two admissable physical states, i.e., $P_A^{\pm}(\mathbf{x})$ and $P_B^{\pm}(\mathbf{x})$ represent two acoustic one-way wavefields (for instance two seismic experiments after decomposition). The underlying assumptions are that the region between $\Sigma_0$ and $\Sigma_m$ is lossless and source-free and that the medium parameters for state $A$ and state $B$ are identical. Moreover, evanescent waves at $\Sigma_0$ and $\Sigma_m$ are ignored. The latter approximation is essential for obtaining a stable inverse propagator in the next section.

Since complex conjugation reverses the propagation direction, it is seen in equation (10) and in Figure 3 that only waves propagating in opposition interact with each other [compare

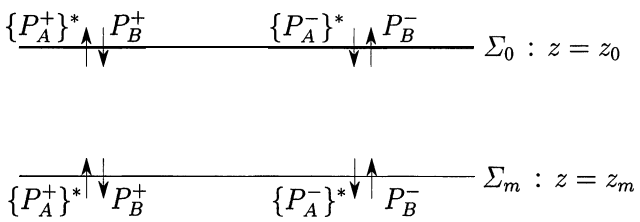


FIG. 3. Configuration for the power recinrocitv theorem (10). The region between $\Sigma_0$ and $\Sigma_m$ is source-free and there are no anelastic losses. Note "that only oppositely propagating waves interact with each other.

with Berkhout and Wapenaar (1989)]. For further interpretation of equation (10), consider the special situation that $P_A^{\pm}(\mathbf{x}) = P_B^{\pm}(\mathbf{x}) = P^{\pm}(\mathbf{x})$. Then equation (10) simplifies to

$$\int_{\Sigma_0} (|P^+(\mathbf{x})|^2 - |P^-(\mathbf{x})|^2)\, d^2\mathbf{x}_H = \int_{\Sigma_m} (|P^+(\mathbf{x})|^2 - |P^-(\mathbf{x})|^2)\, d^2\mathbf{x}_H. \quad (11)$$

This result states that the net incoming power flux through $\Sigma_0$ is equal to the net outgoing power flux through $\Sigma_m$. For this reason, equation (10) is referred to as the power reciprocity theorem for (flux normalized) one-way wavefields.

Using the matrix-vector notation of the previous section, equation (10) can be rewritten as

$$\{\mathbf{P}_A^+(z_0)\}^H\mathbf{P}_B^+(z_0) - \{\mathbf{P}_A^-(z_0)\}^H\mathbf{P}_B^-(z_0) = \{\mathbf{P}_A^+(z_m)\}^H\mathbf{P}_B^+(z_m) - \{\mathbf{P}_A^-(z_m)\}^H\mathbf{P}_B^-(z_m), \quad (12)$$

where $H$ denotes transposition and complex conjugation.

## INVERSE GENERALIZED PRIMARY PROPAGATORS

To derive inverse wavefield propagators, we choose a configuration that is identical to the actual medium between $\Sigma_0$ and $\Sigma_m$ in Figure 3, that is homogeneous above $\Sigma_0$, and scatter-free below $\Sigma_m$ (compare with Figure 1). Moreover, we choose the sources for both states in the upper half-space above $\Sigma_0$. Hence, analogous to equation (3) we may write for state A and state $B$, respectively

$$\mathbf{P}_A^-(z_0) = \underline{\mathbf{X}}_0(z_0, z_0|z_m)\mathbf{P}_A^+(z_0) \quad (13a)$$

and

$$\mathbf{P}_B^-(z_0) = \underline{\mathbf{X}}_0(z_0, z_0|z_m)\mathbf{P}_B^+(z_0), \quad (13b)$$

where $\underline{\mathbf{X}}(z_0, z_0|z_m)$ is the one-way response matrix at $z_0$ for the chosen configuration. Analogous to equation (3b), we may write for $\underline{\mathbf{X}}_0(z_0, z_0|z_m)$:

$$\underline{\mathbf{X}}_0(z_0, z_0|z_m) = \sum_{n=1}^{m} \underline{\mathbf{W}}_g^-(z_0, z_n)\underline{\mathbf{R}}^+(z_n)\underline{\mathbf{W}}_g^+(z_n, z_0). \quad (14)$$

Equation (13) interrelates the wave vectors in the left-hand side of equation (12). For the wave vectors in the right-hand side of equation (12), we write

$$\mathbf{P}_A^+(z_m) = \underline{\mathbf{W}}_g^+(z_m, z_0)\mathbf{P}_A^+(z_0) \quad (15a)$$

and

$$\mathbf{P}_B^+(z_m) = \underline{\mathbf{W}}_g^+(z_m, z_0)\mathbf{P}_B^+(z_0) \quad (15b)$$

and, since the half-space below $\Sigma_m$ is scatter-free

$$\mathbf{P}_A^-(z_m) = \mathbf{P}_B^-(z_m) = \mathbf{O}, \quad (15c)$$

where 0 is the null vector. After substituting equations (13) and (15) into equation (12) we obtain

$$\{\mathbf{P}_A^+(z_0)\}^H(\underline{\mathbf{I}} - \{\underline{\mathbf{X}}_0(z_0, z_0|z_m)\}^H\underline{\mathbf{X}}_0(z_0, z_0|z_m))\mathbf{P}_B^+(z_0) = \{\mathbf{P}_A^+(z_0)\}^H(\{\underline{\mathbf{W}}_g^+(z_m, z_0)\}^H\underline{\mathbf{W}}_g^+(z_m, z_0))\mathbf{P}_B^+(z_0). \quad (16)$$

Since this relation should hold for any choice of $\mathbf{P}_A^+(z_0)$ and $\mathbf{P}_B^+(z_0)$, we obtain

$$\underline{\mathbf{I}} - \{\underline{\mathbf{X}}_0(z_0, z_0|z_m)\}^H\underline{\mathbf{X}}_0(z_0, z_0|z_m) = \{\underline{\mathbf{W}}_g^+(z_m, z_0)\}^H\underline{\mathbf{W}}_g^+(z_m, z_0). \quad (17)$$

For the interpretation of equation (17), we consider the special situation of a horizontally layered medium. Then all matrices are Toeplitz matrices (i.e., constant along the diagonals) and their eigenvalues are plane-wave responses. In particular, the eigenvalues of $\underline{\mathbf{W}}_g^+(z_m, z_0)$ and $\underline{\mathbf{X}}_0(z_0, z_0|z_m)$ are, respectively, the transmission and reflection responses at $z_m$ and $z_0$-related to unit incident plane waves at $z_0$. Consequently, for propagating (i.e., nonevanescent) plane waves the eigenvalues $\lambda_W$ of $\{\underline{\mathbf{W}}_g^+\}^H\underline{\mathbf{W}}_g^+$ quantify the energy of the flux normalized transmission response at $z_m$ (i.e., of the downward propagating generalized primary) and the eigenvalues $\lambda_X$ of $\underline{\mathbf{X}}_0^H\underline{\mathbf{X}}_0$ quantify the energy of the flux normalized reflection response at $z_0$ (i.e., the scattering loss of the generalized primary). Note that $0 \le \lambda_W \le 1$ and $0 \le \lambda_X \le 1$. Moreover, because of equation (17) we have $1 - \lambda_X = \lambda_W$, which formulates conservation of energy.

We return to the arbitrary inhomogeneous situation. Equation (17) can be rewritten as

$$\underline{\mathbf{F}}_g^+(z_0, z_m)\underline{\mathbf{W}}_g^+(z_m, z_0) = \underline{\mathbf{I}}, \quad (18)$$

with

$$\underline{\mathbf{F}}_g^+(z_0, z_m) = (\underline{\mathbf{I}} - \{\underline{\mathbf{X}}_0(z_0, z_0|z_m)\}^H\underline{\mathbf{X}}_0(z_0, z_0|z_m))^{-1}\{\underline{\mathbf{W}}_g^+(z_m, z_0)\}^H. \quad (19)$$

In the following, we call $\underline{\mathbf{F}}_g^+(z_0, z_m)$ the modified matched filter for inverse extrapolation of the downgoing generalized primary. The modified matched filter $\underline{\mathbf{F}}_g^-(z_m, z_0)$ for the upgoing generalized primary follows by applying reciprocity relation (8c). Compared with the usual approximation for flux normalized primary wavefields,

$$\underline{\mathbf{F}}_p^+(z_0, z_m) = \{\underline{\mathbf{W}}_p^+(z_m, z_0)\}^H, \quad (20c)$$

equation (19) shows that the modified matched filter involves a correction term that can be derived from the data: $\underline{\mathbf{X}}_0^H\underline{\mathbf{X}}_0$ represents a multidimensional cross-correlation of the reflection measurements related to the region between $z_0$ and $z_m$ [see equation (14)], deconvolved for the source spectrum [analogously to equation (6)]. It is the frequency-domain equivalent of a correlation along the time axis as well as along the horizontal $x$- and y-axes. Since the correction term in equation (19) is not a scalar but a matrix it takes the angle-dependency of the dispersion effects into account. To avoid matrix inversion, which is computationally unattractive and which may become unstable when $\lambda_X = 1$, we use a Neumann expansion for the correction term. For the kth order approximation we obtain

$$\{\underline{\mathbf{F}}_g^+(z_0, z_m)\}^{(k)}$$

$$= \sum_{j=0}^{k} (\{\underline{\mathbf{X}}_0(z_0, z_0|z_m)\}^H \underline{\mathbf{X}}_0(z_0, z_0|z_m))^j \{\underline{\mathbf{W}}_g^+(z_m, z_0)\}^H, \quad (21)$$

[compare with our surface related multiple elimination scheme, see Verschuur et al. (1992)]. The convergence speed depends on the eigenvalues $\lambda_X$ of $\underline{\mathbf{X}}_0^H \underline{\mathbf{X}}_0$. For low propagation angles these eigenvalues are small, implying a fast convergence. For high propagation angles the convergence is slower. For very high angles, total reflection may occur so that $\lambda_X = 1$ and no convergence is reached at all. In practice this series expansion is terminated after a limited number of terms, meaning that the low propagation angles are more accurately handled than the high angles. An efficient implementation of this expression is the subject of current research.

Equation (21) was originally derived for inverse wavefield extrapolation through macro models with large contrasts (Wapenaar and Berkhout, 1989, Chapter IX). Herman (1992) used an expression similar to equation (17) to derive an inverse propagator completely from the reflection response, under the assumption that the dispersion effects are minimum phase. For our purpose (3-D prestack migration in arbitrarily inhomogeneous media), we prefer not to rely on a minimum phase assumption. $\underline{\mathbf{X}}_0^H \underline{\mathbf{X}}_0$ may be derived from the reflection measurements (as mentioned before) whereas $\underline{\mathbf{W}}_g^+(z_m, z_o)$ is defined preferably in an extended macro model. This yields a robust and stable inverse propagator.

When anelastic losses also play a role, this propagator needs to be modified further. Assuming that the anelastic losses do not depend on the propagation angle, the latter modification can be accomplished by a time-variant deconvolution process. Further discussion of this is beyond the scope of this paper.

## EXAMPLES

To illustrate the limitations of the matched filter and the potential of the modified matched filter we consider a 1-D model. For this situation, all matrix equations given in this paper simplify to scalar equations in the ray parameter-frequency $(p, \omega)$ domain.

Figure 4 shows a 1-D acoustic medium consisting of 15 000 layers with a thickness of 10 cm each. The statistics of the fine layering are described by fractal Brownian motion (Walden and Hosken, 1985; Herrmann, 1992). The average velocity $\bar{c}$ equals 2500 m/s and the average density $\bar{\rho}$ equals 2500 kg/m$^3$. The standard deviations for the velocity and density are 453 m/s and 418 kg/m$^3$, respectively. We modeled the upgoing plane waves, propagating from the bottom to the top of the configuration. The ray parameter $p$ ranges from 0.0 to $0.8/\bar{c}$; hence, the propagation angle ranges from 0° to 53°. The lower frame in Figure 4 shows the modeling input at the bottom of the configuration. It will serve as a reference for the inverse extrapolation output. The upper frame in Figure 4 shows the modeling output at the top of the configuration (note that the angle-dependent scattering losses are significant, particularly in the last two traces, where tunneling occurs). This result will serve as the input for the inverse extrapolation experiments.

Figure 5 shows the setup for inverse extrapolation. The upper frame again shows the modeling result of Figure 4; the lower frame shows the inverse extrapolation result. For this particular example, the inverse extrapolation was done with the primary propagator $\underline{\mathbf{F}}_p^- = \{\underline{\mathbf{F}}_p^+\}^T$, with $\underline{\mathbf{F}}_p^+$ defined in equation (20). In the ray parameter-frequency domain, this is a simple phase-shift propagator, hence, the angle-dependent amplitude and phase distortions are not accounted for. Figure 6 shows the results of applying thep, o-domain version of the generalized primary propagator $\underline{\mathbf{F}}_g^{-(k)} = \{\underline{\mathbf{F}}_g^{+(k)}\}^T$, with $\underline{\mathbf{F}}_g^{+(k)}$ defined in equation (21). Any of these results (for $k = 0$, 1, 5 or 100) replaces the lower frame in Figure 5. Figure 6a $(k = 0)$ was obtained with the matched filter modeled in the actual medium. The results are zero-phase, but the AVA behavior is worse than in Figure 5, because the amplitude decay occurred twice (during modeling and during inverse extrapolation).

Figures 6b, 6c, and 6d were obtained with the modified matched filter, taking, respectively, one, five, and one hundred terms of the Neumann series into account. The last result in particular (Figure 6d) shows a very good amplitude recovery

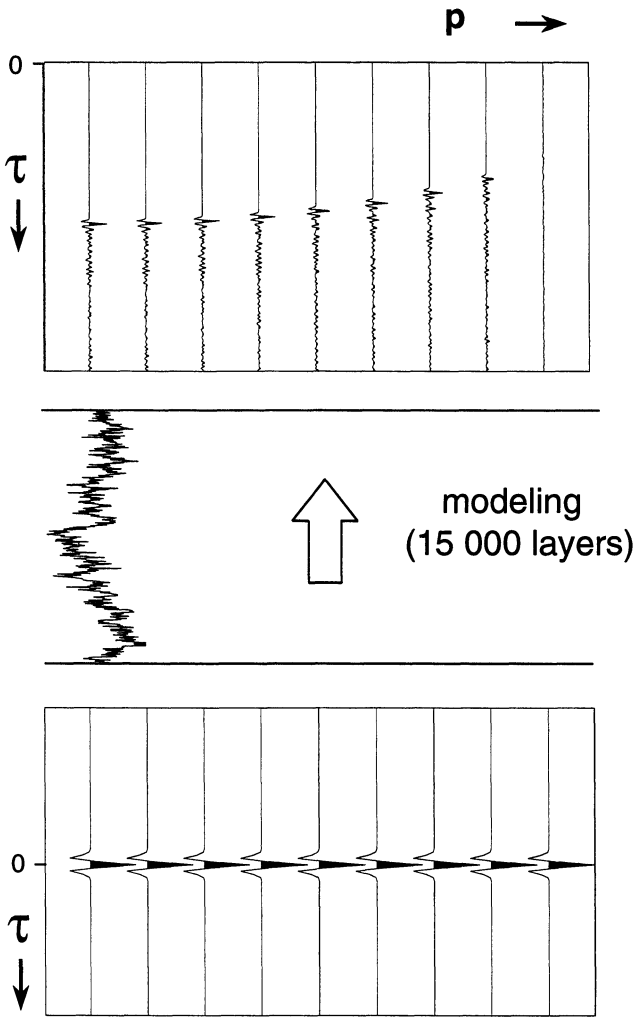


FIG. 4. Plane-wave transmission response of a 1-D acoustic medium (the time axis in the upper frame is different from that in the lower frame).

up to very high propagation angles (compare with the lower frame of Figure 4). Moreover, this result appears to be nearly noise-free, despite the noisy coda in the input data. Apparently, the modified matched filter also accounts for the long period internal multiples. In practice, however, it is not feasible to model the generalized primary propagator in the actual medium, including the correct details of the fine layering. Therefore we consider another experiment that is closer to the reality of seismic practice, that is, we replace the matched filter $\{\underline{\mathbf{W}}_g^+\}^H$ in equation (21) by its parameterized version $\{\bar{\underline{\mathbf{W}}}_g^+\}^H$. The relevant parameters are the parameters of the fractal Brownian motion process that underlies the finely layered medium in Figure 4. In practice, these parameters can be derived from a well log, from vertical seismic profile (VSP) measurements, or (using power reciprocity) directly from the deconvolved reflection measurements. For a further discussion on the estimation of these parameters, see Herrmann (1994).

As a result of the parameterization, for this experiment $\bar{\underline{\mathbf{W}}}_g^+$ contains the dispersed primary but not the detail in the coda. The term $\underline{\mathbf{X}}_0^H \underline{\mathbf{X}}_0$ in equation (21) is again defined in the actual medium, since in practice it can be obtained from the measured data. Figure 7 shows the results of applying the p, o-domain version of $\bar{\underline{\mathbf{F}}}_g^{-(k)} = \{\bar{\underline{\mathbf{F}}}_a^{+(k)}\}^T$, for $k$ = 0, 1, 5, and 10. Comparing these results with Figure 6, we observe that approximately the same amplitude recovery is achieved. However, the results in Figure 7 appear to be more noisy because the long period internal multiples are not accounted for. Figure 7d (k = 10) is the result that would typically be

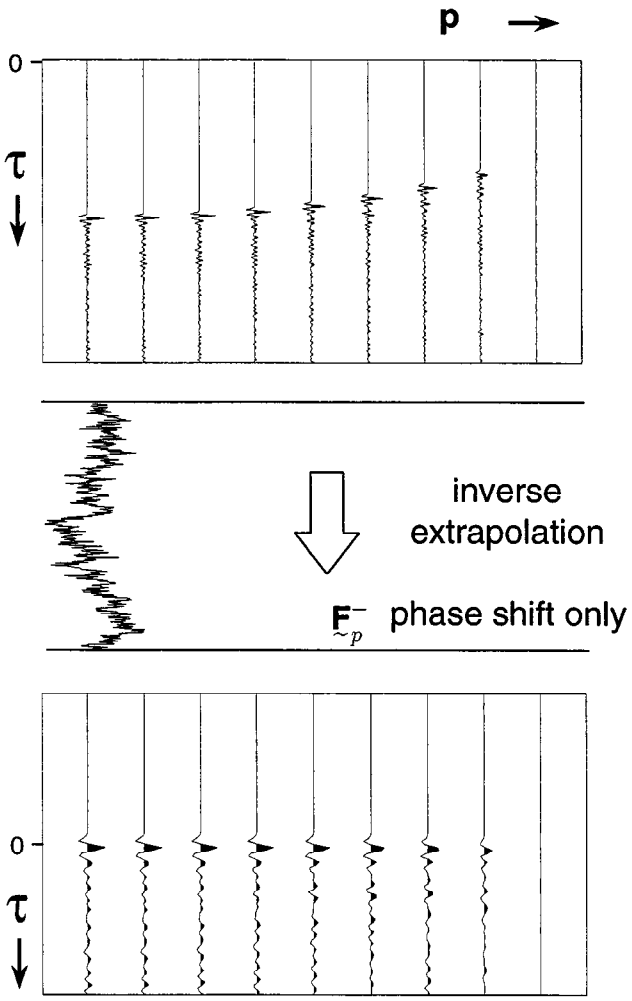


FIG. 5. Setup for inverse extrapolation experiments (here a simple phase-shift extrapolation was applied).

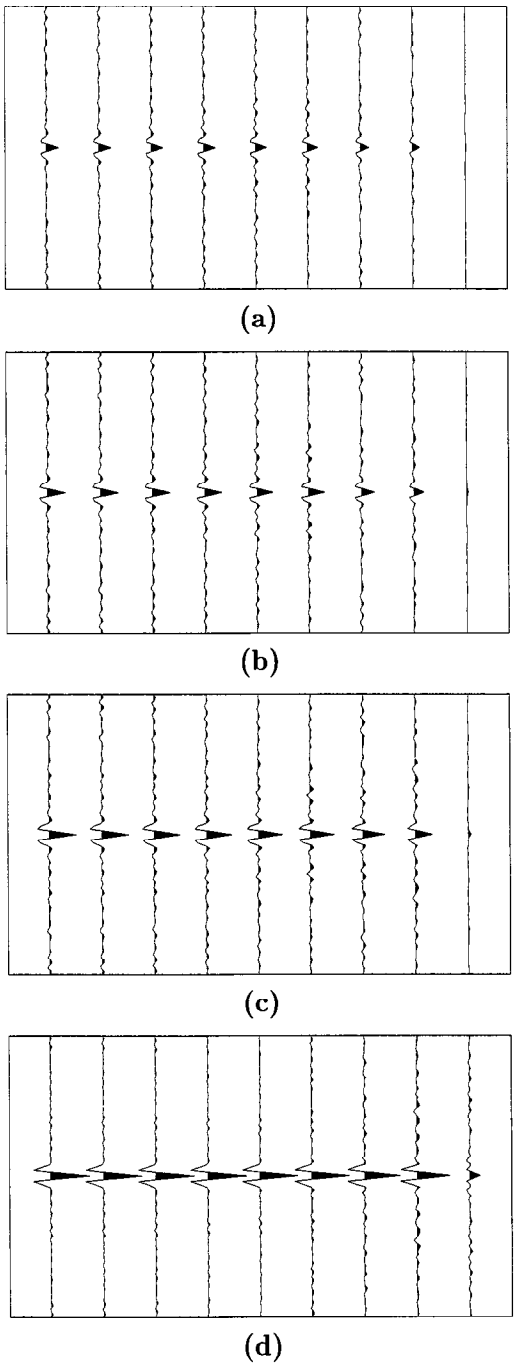


FIG. 6. Inverse extrapolation results using (a) matched filter, (b) modified matched filter with one correction term, (c) idem, with five correction terms, (d) idem, with one hundred correction terms. The matched filter and the correction terms are both defined in the actual medium.

obtained in practice. Note that the improvement with respect to the matched filter result (Figure 7a) is significant again.

## CONCLUSIONS

We have derived an inverse wavefield propagator that accounts for the scattering losses of a generalized primary propagating through a 3-D inhomogeneous medium with fine layering [equation (21)]. This propagator is given by the matched filter $\{\underline{\mathbf{W}}_g^+\}^H$, premultiplied by a correction term that can be derived from the reflection measurements. $\underline{\mathbf{W}}_g^+$ may either be parameterized or it may be defined in an extended macro model. With a 1-D example, we have illustrated that this modified matched filter properly accounts for the angle-dependent amplitude and phase distortions related to the scattering losses.

By integrating the proposed inverse propagator in a prestack migration scheme [equations (6) through (9)], one may expect to obtain a nondispersed image with correct AVA behavior.

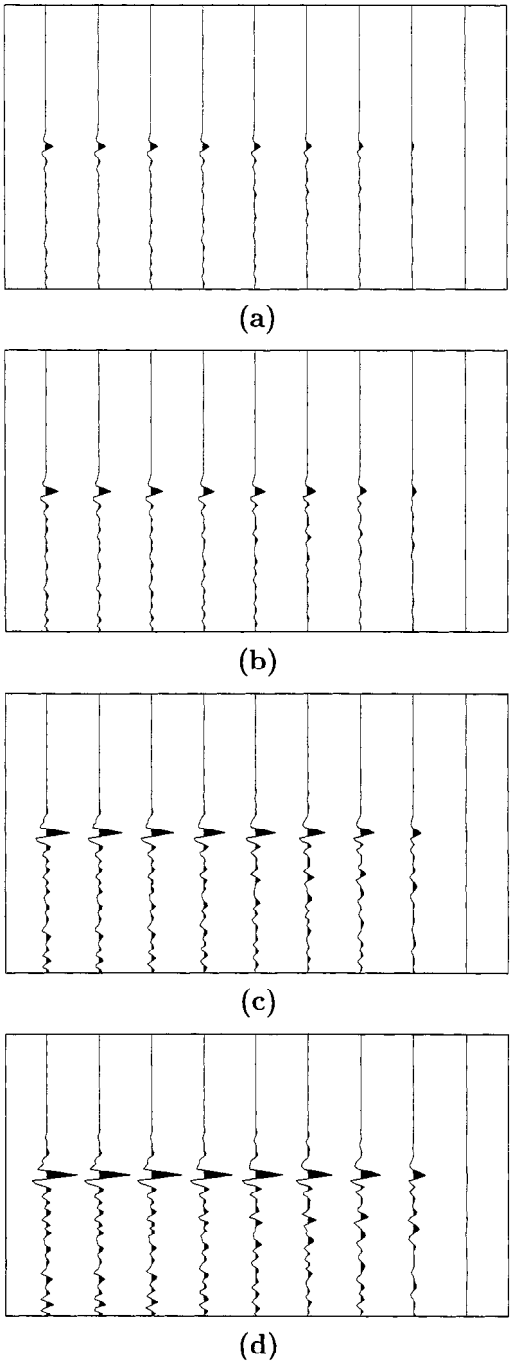


**FIG.** 7. Inverse extrapolation results using (a) matched filter, (b) modified matched filter with one correction term, (c) idem, with five correction terms, (d) idem, with ten correction terms. The matched filter has been parameterized; the correction terms are again defined in the actual medium.

## ACKNOWLEDGMENTS

The authors thank Dr. K. Pann and the anonymous reviewers for their constructive remarks.

## REFERENCES

Berkhout, A. J., 1982, Seismic migration: Elsevier Science Publ. Co., Inc.

Berkhout, A. J., and Wapenaar, C. P. A., 1989,One-way versions of the Kirchhoff integral: Geophysics, 54, 460 - 467.

Bojarski, N. N., 1983, Generalized reaction principles and reciprocity theorems for the wave equations and the relationship between the time-advanced and time-retarded fields: J. Acoust. Soc. Am., 74, 281-285.

Burridge, R., and Chang, H. W., 1989, Multimode, one-dimensional wave propagation in a highly discontinuous medium: Wave Motion, **11, 231-249.**

de Bruin, C. G. M., Wapenaar, C. P. A., and Berkhout, A. J., 1990, Angle-dependent reflectivity by means of prestack migration: Geophysics, 55, 1223-1234.

de Hoop, A. T., 1988, Time-domain reciprocity theorems for acoustic wavefields in fluids with relaxation: J. Acoust. Soc. Am., 84, 1877-1882.

Fokkema, J. T., and van den Berg, P. M., 1993, Seismic applications of acoustic reciprocity: Elsevier Science Publ. Co., Inc.

Herman, G. C., 1992, Estimation of the inverse acoustic transmission operator of a heterogeneous region directly from its reflection operator: Inverse Problems, 8, 559-574.

Herrmann, F. J., 1992, The effect of detail on wave propagation: Towards an improved macro model parameterisation: M. Sc. thesis, Delft University of Technology.

— 1994, Scaling of the pseudo primary, analyzed by the wavelet transform: 64th Ann. Internat. Mtg., Soc. Expl. Geophys., Expanded Abstracts, 1049-1052.

Herrmann, F. J., and Wapenaar, C. P. A., 1993, Wave propagation in finely layered media, a parametric approach: 63rd Ann. Internat. Mtg., Soc. Expl. Geophys., Expanded Abstracts, 909-912.

Hubral, P., Treitel, S., and Gutowski, P. R., 1980, A sum autoregressive formula for the reflection response: Geophysics, 45, 1697-1705.

O'Doherty, R. F., and Anstey, N. A., 1971, Reflections on amplitudes: Geophys. Prosp., 19, 430-458.

Resnick, J. R., Lerche, I., and Shuey, R. T., 1986, Reflection, transmission, and the generalized primary wave: Geophys. J. Roy. Astr. soc., 87, 349-377.

Ursin, B., 1983, Review of elastic and electromagnetic wave propagation in horizontally layered media: Geophysics, 48, 1063-1081.

Verschuur, D. J., Berkhout, A. J., and Wapenaar, C. P. A., 1992, Adaptive surface-related multiple elimination: Geophysics, 57, 1166-1177.

Walden, A. T., and Hosken, J. W. J., 1985, An investigation of the spectral properties of primary reflection coefficients: Geophys. Prosp., 33, 400-435.

Wapenaar, C. P. A., 1996, Inversion versus migration: A new perspective to an old discussion: Geophysics, 61, 804- 814.

Wapenaar, C. P. A., and Berkhout, A. J., 1989, Elastic wavefield extrapolation: Elsevier Science Publ. Co., Inc.

Wapenaar, C. P. A., and Grimbergen, J. L. T., 1996, Reciprocity theorems for one-way wavefields: Geoph. J. Int., 127.

Wapenaar, C. P. A., Slot, R. E., and Herrmann, F. J., 1994, Towards an extended macro model, that takes fine-layering into account: J. Seis. Expl., 3, 245-260.

Wapenaar, C. P. A., van der Leij, T. S., and van Wijngaarden, A. J., 1995, AVA and the effects of interference: 65th Ann. Internat. Mtg., Soc. Expl. Geophys., Expanded Abstracts, 1125-1128.

## APPENDIX

### POWER RECIPROCITY FOR TWO-WAY AND ONE-WAY WAVEFIELDS.

In this Appendix, we derive equation (10) for an arbitrarily inhomogeneous medium in the configuration of Figure 3, with the restriction that no lateral variations of the medium parameters occur at $\Sigma_0$ and $\Sigma_m$. A more general derivation without this restriction can be found in Wapenaar and Grimbergen (1996).

Following de Hoop (1988), we consider two acoustic states $\{P_A, V_A\}$ and $\{P_B, V_B\}$, where P is the acoustic pressure and V the particle velocity, with both in the space-frequency domain. In a source-free volume $\mathcal{V}$, these acoustic states satisfy the following equations:

$$\nabla P_{A,B} = -j\omega\varrho \mathbf{V}_{A,B} \tag{A-1}$$

and

$$\nabla \cdot \mathbf{V}_{A,B} = -\frac{j\omega}{K} P_{A,B}, \tag{A-2}$$

where $\varrho$ is the mass density and $K$ the compression modulus. Note that we have assumed that the medium parameters in state A are identical to those in state $B$. If we also assume that there are no anelastic losses, then $\varrho$ and $K$ are real. Now it is easily seen from equations (A-l) and (A-2) that the following identity holds in $\mathcal{V}$:

$$\nabla \cdot (P_A^* \mathbf{V}_B + \mathbf{V}_A^* P_B) = 0. \tag{A-3}$$

Applying the Gauss theorem thus yields the following power reciprocity theorem for two-way wavefields:

$$\oint_{\Sigma} (P_A^* \mathbf{V}_B + \mathbf{V}_A^* P_B) \cdot \mathbf{n}\, d^2\mathbf{x} = \int_{\mathcal{V}} \nabla \cdot (P_A^* \mathbf{V}_B + \mathbf{V}_A^* P_B)\, d^3\mathbf{x} = 0, \tag{A-4}$$

where $\Sigma$ is the surface enclosing $\mathcal{V}$ and n is the outward pointing normal vector on $\Sigma$. When the medium in $\mathcal{V}$ is ***piecewise*** continuous, then an equation similar to (A-4) applies to each of the continuous regions within $\mathcal{V}$. Summing over these regions again yields equation (A-4) for the total volume and the outer boundary, since the surface integrals cancel at the inner boundaries.

Next, we replace the closed surface $\Sigma$ by two horizontal surfaces $\Sigma_0$ and $\Sigma_m$ at $z = z_0$ and $z = z_0$, respectively, and a cylindrical surface with a vertical axis through the origin and radius $r \to \infty$. The contribution of the integral over this cylindrical surface vanishes (the area of this surface is proportional to $r$, the integrand is proportional to $1/r^2$ for $r \to \infty$). Since the normal vectors on $\Sigma_0$ and $\Sigma_m$ point in opposite directions, we obtain

$$\int_{\Sigma_0} (P_A^* V_{z,B} + V_{z,A}^* P_B)\, d^2\mathbf{x}_H = \int_{\Sigma_m} (P_A^* V_{z,B} + V_{z,A}^* P_B)\, d^2\mathbf{x}_H, \tag{A-5}$$

where $\boldsymbol{V_z}$ is the vertical component of V. Our aim is to replace the two-way wavefields in this equation by one-way wavefields. For convenience, from here onward we assume that the medium parameters are laterally invariant at $\Sigma_0$ and $\Sigma_m$. We introduce $\tilde{P}$ and $\tilde{V}_z$ as the Radon transforms[2] of $\boldsymbol{P}$ and $V_z$. Applying Parseval's theorem yields

$$\left(\frac{\omega}{2\pi}\right)^2 \int_{\mathcal{R}^2} (\tilde{P}_A^* \tilde{V}_{z,B} + \tilde{V}_{z,A}^* \tilde{P}_B)_{z_0}\, d^2\mathbf{p} = \left(\frac{\omega}{2\pi}\right)^2 \int_{\mathcal{R}^2} (\tilde{P}_A^* \tilde{V}_{z,B} + \tilde{V}_{z,A}^* \tilde{P}_B)_{z_m}\, d^2\mathbf{p}, \tag{A-6}$$

where $\mathrm{p} = (p_x, p_y)$, withp, andp, being the ray parameters. At $z_o$ and $z_m$, we may use the following relation between the two-way and one-way wavefields:

$$\begin{pmatrix} \tilde{P} \\ \tilde{V}_z \end{pmatrix}_{A,B} = \begin{pmatrix} \tilde{L}_1 & \tilde{L}_1 \\ \tilde{L}_2 & -\tilde{L}_2 \end{pmatrix} \begin{pmatrix} \tilde{P}^+ \\ \tilde{P}^- \end{pmatrix}_{A,B}, \tag{A-7}$$

where

$$\tilde{L}_1 = \sqrt{\varrho/2q}, \qquad \tilde{L}_2 = \sqrt{q/2\varrho} \tag{A-8}$$

and

$$q^2 = c^{-2} - |\mathbf{p}|^2, \text{ with } c^2 = K/\varrho, \tag{A-9}$$

(see for instance Ursin, 1983). Hence, at $z_0$ and $z_m$ we have

$$\tilde{P}_A^* \tilde{V}_{z,B} + \tilde{V}_{z,A}^* \tilde{P}_B = \tilde{L}_1^* (\tilde{P}_A^+ + \tilde{P}_A^-)^* \tilde{L}_2 (\tilde{P}_B^+ - \tilde{P}_B^-) + \tilde{L}_2^* (\tilde{P}_A^+ - \tilde{P}_A^-)^* \tilde{L}_1 (\tilde{P}_B^+ + \tilde{P}_B^-). \tag{A-10}$$

For the propagating wavefield ($|\mathbf{p}| \le c^{-1}$), we have $\tilde{L}_1^* \tilde{L}_2 = 1/2$. Hence, at $z_0$ and $z_m$ we obtain

$$\tilde{P}_A^* \tilde{V}_{z,B} + \tilde{V}_{z,A}^* \tilde{P}_B = (\tilde{P}_A^+)^* \tilde{P}_B^+ - (\tilde{P}_A^-)^* \tilde{P}_B^-, \text{ for } |\mathbf{p}| \le c^{-1}. \tag{A-11}$$

Assuming that evanescent waves may be ignored (for $|\mathbf{p}| > c^{-1}$ at $z_0$ and $z_m$), upon substitution of equation (A-11) into equation (A-6) we obtain

$$\left(\frac{\omega}{2\pi}\right)^2 \int_{\mathcal{R}^2} \{(\tilde{P}_A^+)^* \tilde{P}_B^+ - (\tilde{P}_A^-)^* \tilde{P}_B^-\}_{z_0}\, d^2\mathbf{p} \approx \left(\frac{\omega}{2\pi}\right)^2 \int_{\mathcal{R}^2} \{(\tilde{P}_A^+)^* \tilde{P}_B^+ - (\tilde{P}_A^-)^* \tilde{P}_B^-\}_{z_m}\, d^2\mathbf{p}. \tag{A-12}$$

Once again applying Parseval's theorem yields the following power reciprocity theorem for one-way wavefields:

$$\mathbf{I}_{\Sigma_0} \{(P_A^+)^* P_B^+ - (P_A^-)^* P_B^-\}\, d^2\mathbf{x}_H \approx \int_{\Sigma_m} \{(P_A^+)^* P_B^+ - (P_A^-)^* P_B^-\}\, d^2\mathbf{x}_H. \tag{A-13}$$

The approximation sign ($\approx$) denotes that the evanescent waves at $z_0$ and $z_m$ are neglected in this expression. In the text we replace $\approx$ by = when the negligence of evanescent waves is the only approximation.

[2]The Radon transform is a spatial Fourier transform with $k_x$ and $k_y$ replaced by $\omega p_x$ and $\omega p_y$, respectively.